GA–A26098

SPECTRALLY FILTERED FAST IMAGING OF INTERNAL MHD ACTIVITY IN THE DIII-D TOKAMAK

by
J.H. YU, and M.A. VAN ZEELAND

MAY 2008

GENERAL ATOMICS

DISCLAIMER

GA–A26098

SPECTRALLY FILTERED FAST IMAGING OF INTERNAL MHD ACTIVITY IN THE DIII-D TOKAMAK

by
J.H. YU,* and M.A. VAN ZEELAND

This is a preprint of a paper to be presented at the Seventeenth Topical Conference on High Temperature Plasma Diagnostics, May 11-15, 2008, in Albuquerque, New Mexico, and to be published in the *Proceedings.*

*University of California-San Diego, La Jolla, California.

Work supported by
the U.S. Department of Energy
under DE-FG02-07ER54917 and DE-FC02-04ER54698

GENERAL ATOMICS ATOMICS PROJECT 30200
MAY 2008

GENERAL ATOMICS

ABSTRACT

The detailed poloidal structure of internal magnetohydrodynamic (MHD) modes is imaged using broadband visible bremsstrahlung emission from the core of the DIII-D tokamak. Spectral analysis of individual pixel time series recorded by a fast framing camera (up to 26k frames/s at 256×256 spatial resolution) is used to reconstruct 2D images of mode amplitude. Application of this spectrally filtered fast imaging (SFFI) technique reveals spatially extended coherent structures that correspond to a $(m,n) = (1,1)$ kink mode and (2,1) neoclassical tearing mode rotating in the laboratory frame. The SFFI technique produces images with significantly less noise than images produced with the commonly used background subtraction method. Extension of SFFI to other core MHD events and coherent fluctuations in general is straightforward and could lead to further understanding of core MHD activity in fusion devices.

I. INTRODUCTION

Imaging of fusion plasmas is a growing area of research and provides insight into plasma instabilities, structure, and dynamics. In tokamaks, fast framing visible cameras are used to image turbulence and instabilities in the plasma edge [1–4], record dynamics of dust particles [5–7], and are used for a variety of other studies. 2D Z_{eff} profiles have been inferred by imaging bremsstrahlung emission [8], and MHD activity has been related to single channel infrared [9] and multi-channel x-ray measurements [10] of bremsstrahlung emission; however, 2D imaging of plasma instabilities using visible emission from the core of tokamaks has previously been lacking due to typically low contrast levels, large signal contribution from plasma edge emission, and slow frame rates. Here we present images of fluctuating visible bremsstrahlung emission due to MHD modes in the core of the DIII-D tokamak. The images are obtained by spectrally filtering temporal data from individual pixels using a fast Fourier transform (FFT), and then transforming back to the time domain to reconstruct 2D images of selected Fourier components at each frame. Spectral filtering here refers to the digital filtering process applied to temporal data from each camera pixel and does not refer to optical filtering. This spectrally filtered fast imaging (SFFI) technique can be applied to imaging applications across a variety of disciplines where the goal is to visualize structure from repetitive events in low contrast situations.

II. EXPERIMENTAL SETUP

A Phantom v7.1 12-bit CMOS camera with maximum frame rate of 26k frames/s and spatial resolution of 256×256 pixels is used to image the midplane region of the DIII-D tokamak. Figure 1 shows a plan view of DIII-D and the viewing geometry of the objective lens of the camera system, and the inset shows the view inside the vessel. The camera can store a maximum of 2.1×10^4 frames from one continuous movie covering a duration of 830 ms. For the data presented here, 128 frames are used which cover 5.9 ms. The size of each pixel is 22×22 μm and each pixel images approximately 0.1 cm^2 in the plasma. The camera is located approximately 2 m from the outside of the DIII-D vessel due to space constraints and shielding requirements. The area surrounding the tokamak is extremely noisy, and thermonuclear neutron flux is attenuated by surrounding the camera on all sides by a ~10 cm thick layer of polycarbonate and borated plaster with a 3 cm diameter hole allowing signal light to reach the camera. Magnetic shielding consists of a 3 mm thick layer of proprietary high permeability alloy made by Magnetic Shield Corporation, and 0.5 cm thick lead is used to attenuate gamma and x-rays.

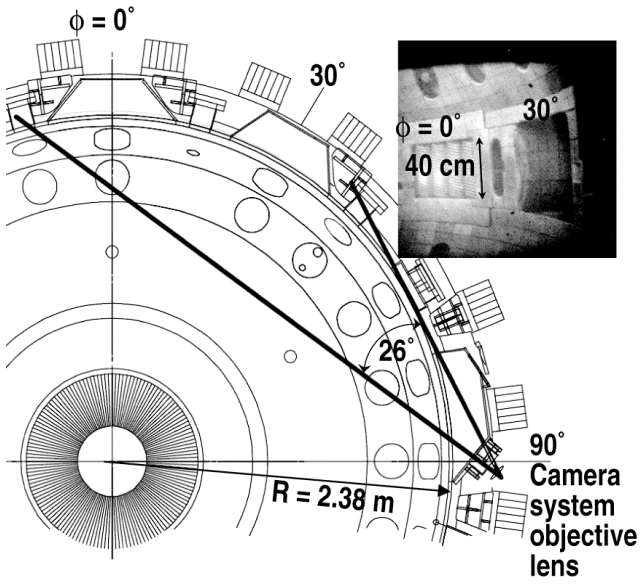

Fig. 1. Plan view of DIII-D tokamak showing the fast camera field of view. The inset shows the camera view inside the vessel.

The fast camera optical system collects light from the plasma through a quartz viewport located 7.6 cm above the plasma midplane. A 12 mm, f/1.2 objective lens focuses the plasma image onto the front face of a 2.7 m coherent fiber bundle composed of 800×1000 individual fiber optic elements each with diameter 8 μm and numerical aperture 0.6. Light coming out of the back of the fiber bundle is focused onto the camera detector. The light throughput is characterized by the étendue (η), and for a single pixel η describes the light emitted from a

pixel-equivalent area into a solid angle Ω subtended by the objective lens, and is given by $\eta = A\Omega = 3\times10^{-6}$ cm^2 sr. The surface radiance of the viewing object multiplied by η is the maximum possible collected signal in photons/s, provided that η is not compromised by geometrical effects or other losses downstream. In our system, signal losses through fibers and at optical surfaces must be taken into account, and thus an annual calibration is performed during maintenance periods by placing a calibrated integrating light source with color temperature 3000 K inside the vacuum vessel. Narrow band (~30 Å) interference filters covering the camera system spectral range of 4500 Å to 9500 Å are used to obtain the camera system spectral response $F(\lambda)$, which peaks at $\lambda_0 = 6900$ Å with $F(\lambda_0) \approx 6\times10^{-9}$ counts/(photons/cm^2 sr). Maintaining the camera system calibration is not trivial, however, because 2.5 MeV neutrons and gamma rays from D-D fusion reactions degrade the optical transmission of the fiber over time. The fiber bundle is removed from the tokamak area when not in use to minimize neutron exposure.

III. OPTICAL DETECTION

The light detected by the camera includes line emission from deuterium atoms and carbon impurities from the graphite wall, continuum bremsstrahlung emission from the hot core of the plasma, and emission from molecular bands. The line emission source region is localized near the plasma edge because in the plasma core (T_e > 1 keV) most of the low-Z elements are fully ionized. Line emission typically dominates continuum emission, and thus to image the core of the plasma one strategy is to use optical filters that select a line-free region of the spectrum [8]. However, to maximize signal, no optical filters are used here. Instead, we show that post-processing the recorded emission signal using the SFFI technique allows core mode structure to be imaged in detail, despite low contrast.

In the core plasma region, the continuum radiation in the visible part of the spectrum is due entirely to bremsstrahlung emission and is given by [11]

$$\varepsilon_B = 2.27 \times 10^{-14} \frac{n_e^2 Z_{eff}}{\lambda T_e^{1/2}} e^{-hc/\lambda T_e} \quad , \tag{1}$$

where electron density n_e is in units of cm^{-3}, wavelength λ is in units of Å, electron temperature T_e is in units of eV, the local emission ε_B is in units of photons/(s cm^3 Å sr), the effective charge is given by $Z_{eff} \equiv \sum_i (n_i Z_i^2)/n_e$ where n_i is the density of ions of charge state Z_i, and a value of 3 is used for the electron free-free transition Gaunt factor. The plasmas studied here have central electron density $n_e = 7 \times 10^{13}$ cm^{-3}, electron temperature $T_e(0) = 1.4$ keV, toroidal magnetic field $B_T = 2.0$ T, central $Z_{eff} \sim 3$–4, yielding a local $\varepsilon_B = 1 \times 10^9$ photons/(s cm^3 sr Å) for wavelengths in the visible spectrum.

To determine how much of the light detected by the camera is due to bremsstrahlung radiation, the local emission ε_B is integrated along each pixel's line-of-sight and is then convolved with the camera spectral response function $F(\lambda)$. The line-of-sight integral yields the bremsstrahlung spectral radiance $R_B(\lambda) = \int \varepsilon_B(\rho,\lambda) dl$, where ρ is the normalized flux surface coordinate proportional to the square root of toroidal flux. The profile $\varepsilon_B(\rho)$ is determined by inverting data from 16 tangentially viewing chords that detect a line-free region of the bremsstrahlung continuum spectrum at 5230 Å with a 30 Å FWHM bandpass [11]; this profile is normalized to $\varepsilon_B(\rho = 0)$ using Eq. (1) and measured plasma parameters. Evaluating the line-of-sight integral yields a bremsstrahlung spectral radiance at $\lambda_0 = 6900$ Å of $R_B(\lambda_0) = 3 \times 10^{11}$ photons/(s cm^2 sr Å), which is roughly equivalent to the bremsstrahlung spectral radiance detected in ASDEX Upgrade in Ref. [12], and is up to 10× higher than that seen in other tokamak plasma discharges [13] and in typical DIII-D discharges, due to high n_e, low T_e, and high Z_{eff}. Using the existing camera system, such high levels of bremsstrahlung emission are required to image core mode activity. The spectral radiance is then convolved with the camera response function to predict the bremsstrahlung count rate I_B detected by the camera, given by $I_B = \int R_B(\lambda) F(\lambda) d\lambda$ in

units of counts/s. We find that in the discharges presented here, visible bremsstrahlung emission accounts for a significant part of the total detected signal I_0 at the magnetic axis, with $I_B / I_0 \approx 0.4$ and approximate uncertainty of a factor of 2 mainly due to uncertainty in $F(\lambda)$.

IV. MODE DETECTION AND SPECTRAL FILTERING

We apply the SFFI technique to images of DIII-D with $(m,n) = (1,1)$ kink and (2,1) neoclassical tearing modes (NTMs), where m and n are the poloidal and toroidal mode numbers, respectively. The (1,1) kink mode is a helical distortion of the central region of the plasma, driven by the peaking of the plasma pressure and current density at the magnetic axis. NTMs are resistive magnetohydrodynamic (MHD) instabilities that occur at high beta. They are destabilized by local reduction of the neoclassical bootstrap current inside a seed magnetic island, and saturate when this driving force is balanced by the "classical" tearing stability parameter Δ' (which here is stabilizing). The study of NTMs is important because NTMs can limit plasma pressure, which in turn limits fusion performance in tokamaks.

Figure 2 shows the spectrum from a Mirnov magnetic pickup coil (solid black line) and the spectrum from 900 camera pixels (red dashed line) imaging the region of the magnetic axis. Both the magnetic perturbation and the camera signals show spectral power peaked at the (1,1) saturated kink mode frequency of 5.3 kHz, indicating that mode information is recorded by the camera even though the mode is difficult to see in the unprocessed images due to lack of contrast. The spectrum from a single pixel also shows power at the mode frequency, but here we present the spectrum from the sum of a group of pixels to show higher mode power for clarity.

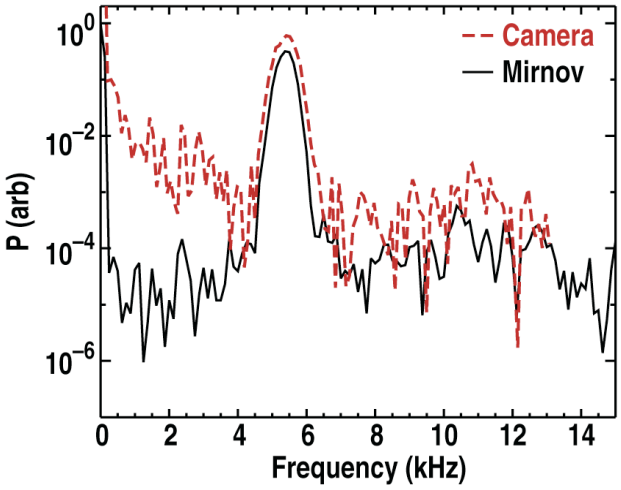

Fig. 2. (Color online) Power spectra of a (1,1) kink mode measured with Mirnov magnetic pickup coils (solid black line) and the fast camera (red dashed line) during shot 131370 at t = 2753 ms.

The SFFI process consists of performing an FFT of the time series data from each camera pixel, keeping spectral power only in a specified frequency range, and transforming back to the time domain. By re-assembling a 2D (x,y) array at each time frame, a movie of selected Fourier components is created. The process is equivalent to applying a digital bandpass filter

to the movie data. For the cases presented here, we choose to retain frequency components based on the mode frequency detected by the magnetic perturbation signal. The SFFI technique can also be used to produce 2D images of the mode Fourier amplitude, the mode phase δ, or the amplitude multiplied by $e^{i\delta}$, which produces an image of the mode structure at one phase of the mode cycle [14]. In addition, SFFI allows isolation of separate mode structures in situations where simultaneous modes exist, provided that the mode frequencies do not overlap.

V. EXPERIMENTAL RESULTS

Figure 3 shows spectrally filtered images of MHD modes compared to images obtained using the classical background subtraction method. We compare to the background subtraction method because it is often used in image processing, in which an average background image created from N_{sub} movie frames is subtracted from each frame. Background subtraction is essentially a high-pass spectral filtering process in which the zero frequency component is eliminated. Both the background-subtracted and the spectrally filtered images are calculated from the same data, represent the same time in the plasma shot, are plotted on the same false-color scale, and $N_{FFT} = N_{sub} = 128$, where N_{FFT} is the number of frames used to calculate the FFT in the spectrally filtered image. The maximum camera frame rate of 26k frames/s is used with an exposure time of 33 μs. Figure 3(a) shows an image of a (1,1) kink mode obtained from the background subtraction method, while Fig. 3(b) shows a spectrally filtered image using frequency components centered at 5.3 kHz with half-width 0.9 kHz in the SFFI process. The camera detects perturbed visible bremsstrahlung emission due to the rotating (m,n) helical mode structure. The mode induces a radial displacement ξ of magnetic field lines, and the fluctuating bremsstrahlung emission is given approximately by $\delta\varepsilon_B \propto \xi \cdot \nabla\varepsilon_B$. The plasma toroidal rotation, in combination with the finite toroidal mode number n, causes an apparent motion of the mode structure in the poloidal plane because the camera views a limited range of toroidal angle. The maximum of

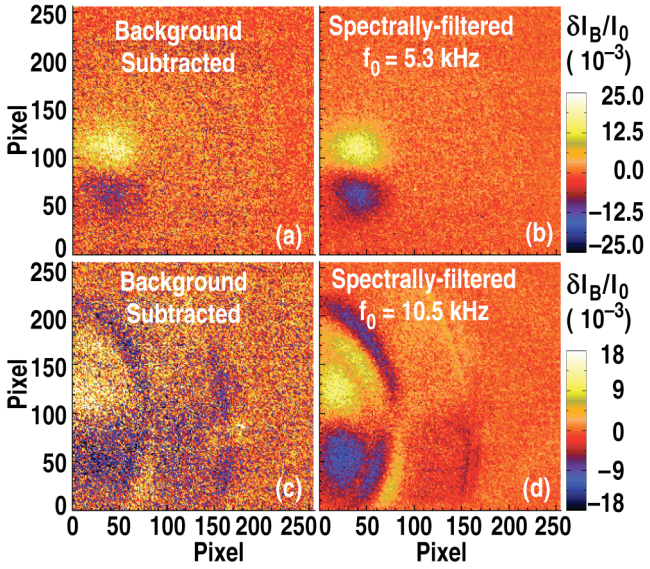

Fig. 3. A (1,1) saturated kink mode imaged using (a) the background subtraction method and (b) the SFFI technique, for the same shot and time as Fig. 2. A (2,1) NTM is shown in (c) and (d) during shot 131364 at t = 2164 ms. The mode structure is easier to identify in the spectrally filtered images compared to the subtraction images.

the perturbed light emission δI_B from the mode represents approximately 2×10^{-3} of the total measured visible light at the magnetic axis. The poloidal mode number m is immediately apparent using both image processing techniques, but the spectrally filtered image appearance is higher quality and allows easier identification of mode structure. We characterize the image quality by the variance, which represents the noise level, and thus lower variance corresponds to higher quality. The variance of the (1,1) kink mode image is smaller by a factor of 3.5 in the spectrally filtered image compared to the background-subtracted image.

A (2,1) NTM from a separate plasma discharge is shown in Fig. 3(c,d), and the mode structure is visualized in detail in the spectrally filtered image using a central frequency of 10.5 kHz with half-width of 0.2 kHz. The field-line displacement here is created by a magnetic island located at the $q = 2$ flux surface, where q is the safety factor. At the island O-point and X-point, flux surfaces are displaced away from and toward the equilibrium $q = 2$ surface, respectively. For the (2,1) NTM case, the variance of the spectrally filtered image is 8.7× smaller than that of the background subtraction image. The larger discrepancy between image-type variances for the (2,1) case compared to the (1,1) case is most likely due to the larger spatial extent of the (2,1) mode in the camera frame compared to that of the (1,1) mode, and the noise is presumably small where the mode exists. We note that the viewing angle of the camera system objective lens was intentionally changed between plasma shots, such that the pixel line-of-sight that is tangent to the magnetic axis is located near pixel value (x,y) = (40,90) for the (1,1) kink mode and near (x,y) = (10,85) for the (2,1) NTM.

To summarize, the SFFI technique produces high quality images with low noise levels for periodic events, and can easily be extended to linear plasma devices or to fields outside of plasma physics. In tokamaks, the unprecedented image quality of core modes allows detailed comparison to modeling, which will be presented elsewhere.

REFERENCES

[1] A. Kirk, B. Koch, R. Scannell, H. R. Wilson, G. Counsell, J. Dowling, A. Herrmann, R. Martin, and M. Walsh, Phys. Rev. Lett. **96**, 185001 (2006).

[2] R. J. Maqueda, G. A. Wurden, D. P. Stotler, S. J. Zweben, B. LaBombard, J. L. Terry, J. L. Lowrance, V. J. Mastrocola, and G. F. Renda, Rev. Sci. Instrum. **74**, 2020 (2003).

[3] S. J. Zweben, R. J. Maqueda, J. L. Terry, and T. Munsat, Phys. Plasmas **13**, 056114 (2006).

[4] J. H. Yu, J. A. Boedo, E. M. Hollmann, R. A. Moyer, D. L. Rudakov, and P. B. Snyder, Phys. Plasmas **15**, 032504 (2008).

[5] A. L. Roquemore, N. Nishino, C. H. Skinner, C. Bush, R. Kaita, R. Maqueda, W. Davis, A. Yu Pigarov and S. I. Krasheninnikov, J. Nucl. Mater. **363**, 222 (2007).

[6] D. L. Rudakov, J. H. Yu, J. A. Boedo, E. M. Hollmann, S. I. Krasheninnikov, R. A. Moyer, S. H. Muller, A. Yu. Pigarov, M. Rosenberg, R. D. Smirnov, W. P. West, R. L. Boivin, B. D. Bray, N. H. Brooks, A. W. Hyatt, C. P. C. Wong, M. E. Fenstermacher, M. Groth, C. J. Lasnier, A. G. McLean, P. C. Stangeby, S. Ratynskaia, A. L. Roquemore, C. H. Skinner, W. M. Solomon "Dust Measurements in Tokamaks," this conference.

[7] J. H. Yu, D. L. Rudakov, A. Yu. Pigarov, R. D. Smirnov, N. H. Brooks, S. H. Muller, W. P. West, "Fast camera imaging of dust in the DIII-D tokamak," to be submitted to J. Nucl. Mater. 2008.

[8] A. Patel, P. G. Carolan, N. J. Conway, and R. J. Akers, Rev. Sci. Instrum. **75**, 4944 (2004).

[9] B. Grek, J. Bartolick, and D. Johnson, Rev. Sci. Instrum. **63**, 4627 (2002).

[10] JET Team (prepared by G. T. A. Huysmans), Nucl. Fusion **39**, 1965 (1999).

[11] D. P. Schissel, R. E. Stockdale, H. St. John, and W. M. Tang, Phys. Fluids **31**, 3738 (1988).

[12] H. Meister, R. Fischer, L. D. Horton, C. F. Maggi, D. Nishijima, C. Giroud, K.-D. Zastrow, and B. Zaniol, Rev. Sci. Instrum. **75**, 4097 (2004).

[13] A. T. Ramsey and S. L. Turner, Rev. Sci. Instrum. **58**, 1211 (1987).

[14] M. A. Van Zeeland, J. H. Yu, M. S. Chu, K. H. Burrell, R. J. La Haye, T. C. Luce, R. Nazikian, W. M. Solomon, and W. P. West, "Spatiotemporal evolution of tearing modes in the DIII-D tokamak through spectrally-filtered fast visible Bremsstrahlung imaging" submitted to Nucl. Fusion Letter 2008.

ACKNOWLEDGMENT

This work supported by the U.S. Department of Energy under DE-FG02-07ER54917 and DE-FC02-04ER54698. The authors would like to thank E.J. Strait and R.J. La Haye for identification of the (1,1) mode.